Life Sciences 218 (2019) 197–204

Contents lists available at ScienceDirect

Life Sciences

journal homepage: www.elsevier.com/locate/lifescie

Columbamine suppresses hepatocellular carcinoma cells through down-regulation of PI3K/AKT, p38 and ERK1/2 MAPK signaling pathways

Zhenwen Lin[a,1], Sheng Li[a,*,1], Peng Guo[b,1], Liyang Wang[c,1], Lisheng Zheng[a], Zixing Yan[a], Xi Chen[a], Zhuqin Cheng[a], Haiyi Yan[b], Cui Zheng[b], Congkuai Zhao[a]

[a] Fuzhou Traditional Chinese Medicine Hospital, Fuzhou 350001, China
[b] Xiyuan Hospital, China Academy of Traditional Medical Sciences, Beijing 100091, China
[c] Beth Israel Deaconess Medical Center, Harvard Medical School, Boston, MA 02215, USA

ARTICLE INFO

Keywords:
Hepatocellular carcinoma (HCC)
Traditional medicine
Columbamine
PI3K/AKT pathway
p38 and ERK1/2 MAPK pathway

ABSTRACT

Hepatocellular carcinoma (HCC) as primary liver cancer in adults is the most common cause led to internal cirrhosis responsible for patients' death, which resulted in nearly a million deaths worldwide on both males and females in the developing and developed countries. Unfortunately, up to date, there are no highly effective treatment of medicine on HCC as lack of comprehensive cellular and molecular mechanism. According to the sources of human ancient history of medicine, traditional medicine could provide unique treatment to discontinue the challenging HCC. In this study, we inspected the effect of Columbamine (Col; C20H21NO5), an alkaloid isolated from calumba, on HCC utilizing three HCC cell-lines *i.e.* SMMC7721, HepG2 and Hep3B. Our data collected from these cell-lines exhibit strong Col suppression on the cell growth accompanying the dosage-dependent suppression, and we further confirmed the suppression on the tumor-growth in animal model. Rational of the Col suppression presents cellular mechanism by limiting the proliferation and colony formation of the cells marked with decreased expression of PCNA. Meanwhile decreases of migration indicated with increasing expression of E-cadherin and decreasing expression of N-cadherin, and of invasion labelled with decreasing expressions of MMP2 and MMP9, are accompanying the Col suppression along with the Col promoted apoptosis of the tumor cells. This programmed cell death marketed with cleaved Caspase 3 plus PAPR proteins, up-regulation of BAD and down-regulation of BCL2 is linked the Col suppression to unique calcium-related pathways. Our results unveiled that the Columbamine suppression on HCC based on the traditional medicine are clearly associated with PI3K/AKT, p38 and ERK1/2 MAPKs signaling pathways and guide further research orientation for developing the Col medicine against hepatocellular carcinoma.

1. Introduction

Hepatocellular carcinoma (HCC) is primary liver cancer in adults and the most common original cause which relates to internal cirrhosis leading to patients' death. HCC is one of the most life-threatening tumors on both males and females in the developing and developed countries which caused almost a million deaths worldwide annually including half amount of the deaths in China [1–3]. Currently, approaches of diagnosis and evaluation on HCC involved with ultrasound, CT scan and MRI imaging, and blood test plus gold-standard of pathological biopsy of the tumor with histopathologic confirmation. Recently, the most routine evaluation approach follows guidelines published by the American Association for the Study of Liver Diseases [4]. However, this evaluation controlled by following the guidelines could not provide high percentage confident specificity at diverse sensitivity with the tumor marker alpha-fetoprotein (AFP) [5]. Compound diagnosis cooperated AFP and the medical imaging can increase the sensitivity from 60% up to 79% accompanied with 97% of specificity [5,6].

Currently, the most effective treatment for HCC patients is surgical resection to remove the HCC with high sensitivity as result after diagnosis. But this approach only can be carried on sufficient functional liver but not on cirrhotic livers, which is essential to maintain normal physiology with overall recurrence rate of 50–60% [7,8]. Because of the HCC complexity of evaluation and treatment on a single large tumor and small multiple tumors in addition of non-defined tumor with an infiltrative growth pattern, furthermore investigation on their

* Corresponding author.
E-mail addresses: sanleeemailftc@163.com (S. Li), lwang@bidmc.harvard.edu (L. Wang).
[1] Equal contributors.

https://doi.org/10.1016/j.lfs.2018.12.038
Received 30 November 2018; Received in revised form 18 December 2018; Accepted 20 December 2018
Available online 21 December 2018

molecular mechanism of HCC tumorigenesis is essential for confronting challenge from the life-threatening HCC.

Columbamine (Col; C20H21NO5) is an alkaloid first found in calumba, which can be isolated from many plants such as Coptis chinensis Franch, Fibraurea tinetoria Lour and *Berberis thunbergii* DC and catalyzed with columbamine oxidase to produce berberine. It was approved that columbamine has low cytotoxicity and functions a suppressor on the proliferation and neovascularization of U2OS cells, a stable metastatic osteosarcoma cell line [9]. A recent work claimed that columbamine presents non-cytotoxic to human dermal fibroblasts (HDF) but exhibited cytotoxic effect against B16-F10 melanoma cells and HepG2 cells [10,11], and induce up-regulation of low density lipoprotein receptor [12]. Recently, some analysis summarized calcium signaling pathways tightly related to tumorigenesis through MARK pathway [13–15], Ca channel pathway, and CaSR/IP3R membrane integrated proteins [13,16–18]. In order to obtain more information for its clinic application on hepatocellular carcinoma, in this study, we inspected effect of columbamine using *in vitro* culture system under different dosage of the drug. Our data approved that Col affects cultured HCC cells including SMMC7721, HepG2 and Hep3B on their cell behaviors by inhibiting their proliferation and migration, and inducing apoptosis. Furthermore we approved that the effects on three cell lines molecularly associate with down-regulation of PI3K/AKT, p38 and ERK1/2 MAPKs signaling pathway accompanying with intracellular calcium. The columbamine suppression was also confirmed on subcutaneous tumor growth in nude mice tumor model produced with SMMC7721 cells.

2. Methods and materials

2.1. Cell cultures and colony formation assay

Hepatocellular carcinoma including SMMC7721, HepG2 and Hep3B cell lines were used in the study and grown at 37 °C in a humidified incubator with 5% CO_2. Cells were cultured in medium (pH 7.4, Invitrogen) supplemented with 10% fetal bovine serum (FBS, Invitrogene), 100 U/ml penicillin and 100 μg/ml streptomycin (1% P/S, Biochem, USA) [19]. The cultured cells were treated with 0 μM, 10 μM, 20 μM, 30 μM, 40 μM and 50 μM Col for different time, and then stained with crystal violet for further observation. SMMC7721 cells were cultured in RPMI 1640 Medium, GlutaMAX™ Supplement (ATCC, Cat#. 61870036), and HepG2/Hep 3B cells maintained in Eagle's Minimum Essential Medium (ATCC Cat#. 30-2003) along with 10% FBS.

In agar assay for colony formation, 1–4 × 10^4 SMMC7721 cells were seeded in a layer of 0.4% agar colony formation medium [20]. The colonies were treated with DMSO, 0 μM, 30 μM, 40 μM and 50 μM Col and then counted for statics analysis.

2.2. Tumorigenesis on nude mice

Nude mice (Animal Core facility of the 2nd Military University School of Medicine) in this study were maintained on the standard condition (25 °C, 12 h light/dark cycle). [21] Male or female mice (n = 48, 12 mice in each group) were divided into 4 groups. SMMC7721 cell lines were injected to subcutaneous tissues of these mice with 5 × 10^6 cells each animal. After injection, different Col doses (5, 10 and 20 mg/kg) were applied by gavage in these *Nude Mouse* for 21 days and the tumor sizes of each mouse were measured every 3 days from the 7 day to the 21 day. All animal maintenance and experiments were carried out in accordance with protocol approved by the Animal Care and Use Committee of Beijing for Animal Use of Universities in P.R. China.

2.3. Western blotting and antibodies

The cultured cells and colony cells were harvested and washed twice with ice-cold phosphate buffered saline (PBS). Then the cells were lysed with ice-cold RIPA buffer (Shanghai, China) in presence of protease inhibitors (Sigma, USA). The concentration of total proteins in cell lysate was detected, and then the cell lysate were mixed in proportion with protein loading buffer. After heated at 100 °C for 5 min, the samples were separated on SDS-polyacrylamide gels and the proteins were transferred to a polyvinylidene difluoride (PVDF) membrane. Then the membranes were blocked with 5% non-fat milk dissolved by T-BST at 4 °C overnight and followed by the incubation of primary antibody at room temperature for 2 h. After washing three times with T-BST (20 min for each time), the membrane were then incubated with horseradish peroxidase linked secondary antibody at room temperature for 2 h, and the enhanced chemiluminescence detection system (Roch Ltd., USA) were carried out for protein expression detection. [22].

The primary antibodies used in our experiments were purchased from CST including GAPDH (Cat# 5174), PCNA (Cat#13110), E-cadherin (Cat#14472 s), N-Cadherin (Cat#13116), MMP2 (Cat#40994), MMP7 (Cat#71031) Caspase3 (Cat# 9662), Cleaved caspase3 (Cat#9664), PAPR (Cat#9532), Cleaved PAPR (Cat#5625), BCL2 (Cat#2872), BAD (Cat#9239), AKT (Cat#4685), p-AKT(Ser473) (Cat#4060, CS), p-AKT(Thr308) (Cat#13038), PTEN (Cat#9559), p38 (Cat#8690), ERK1/2 (Cat# 9194), p-p38 (Cat#4511) and p-ERK1/2 (Cat# 4370). The secondary antibodies used in the study including anti-rabbit IgG (H + L) (Cat#4414) and anti-mouse IgG (H + L) (Cat#4410) were purchased from CST as well.

2.4. Wound-healing approach

The wound-healing approach was carried out as previously described for migration detection of SMMC7721 and HepG2 cells. The cells were seeded in trans-well plates at a density of 10^5 cells per well and then the confluent cells were gently scratched across the whole diameter of the plates with a pipette tip. Fresh medium was used to rinse the cells for removing the cellular debris. Then 30, 40 and 50 μM Col were applied for treatment and the other wells were set as control. The scratched spaces on dish were observed and document immediately after wounding, and this operation was repeated again in 24 h. The images of wounded area were captured with Ob-A1 Zeiss microscopy [23,24].

2.5. Trans-well migration and invasion analysis

trans-Well assays were performed to detect capabilities of migration and invasion of SMMC7721 cells under the treatment of 30, 40 and 50 μM Col. The cells were suspended and diluted in serum-free medium, and then seeded in the upper chambers (Corning Costar, Acton, MA, USA) with (for migration assays) or without (for the invasion assays) EMC. Then medium with 10% FBS was added to the lower chamber. After incubation for required hours, the cells moving to the lower chambers were gently fixed with 4% paraformaldehyde (PFA) for 5–10 min and then stained with 0.5% crystal violet solution at room temperature for 30 min, followed by washing twice with PBS. The stained cells were observed under Ob-A1 Zeiss microscopy and counted with manufactured software [25].

2.6. Apoptosis detection

To detect the apoptosis of SMMC7721 cells after treatments with 30, 40 and 50 μM Col, Hoechst 33258 staining and Annexin V/PI staining were performed. For Hoechst 33258 staining, cells were cultured on a sterile cover slip in culture plates and treated with different Col concentration. After treatment for 24 h, the cells were fixed with 4% PFA for 10 min and then washed twice with PBS. The cells were stained with 5 mg/L of Hoechst 33258 (Leagene Ltd., Beijing, China) and repeated washing once with PBS. The stained samples were observed with A1 Zeiss microscopy.

For Annexin V/PI staining, after the treatment with Columbamine for 24 h, cells were collected and washed twice with PBS. Then, according the procedure of annexin-V FITC apoptosis kit (BD, Pharmingen, USA), the cells were re-suspended in binding buffer and stained with FITC Annexin V and 5 μL propidium iodide (PI) at room temperature (25 °C) for 30 min in the dark. After added another 100 μL 1× binding buffer, the apoptotic cells was quantified [26].

2.7. Imaging J and statics analysis

The crystal violet staining images were documented with the Ob-A1 Zeiss microscopy using manufacturer software. Images were analyzed with Image J, and the densities of stained cells were calculated. The experiment data were statistically analyzed with SPSS and presented as mean ± SEM. The analysis of variance (ANOVA) and *t*-test were used for the statistical significance analysis. p values < 0.05 and 0.01 were considered statistically significant.

3. Results

To inspect pharmacological function of columbamine in hepatocellular carcinoma, we applied three different cell-lines including HCC SMMC7721, HepG2 and Hep3B at 5 different Col concentrations to evaluate its role on cellular mechanism. Sequentially, possible related pathways were detected and deciphered PI3K/AKT, p38 and ERK1/2 MAPKs signaling pathway as the most involved molecular mechanism for comprehending columbamine suppression function on HCC. Furthermore, an animal model was employed to confirm the function on tumorigenesis.

3.1. Columbamine inhibits the proliferation from HCC cell level to tumorigenesis in animal

The columbamine at concentration of 10 μm, 20 μm, 30 μm, 40 μm and 50 μm was applied in the medium for culture of SMMC7721, HepG2 and Hep3B cell lines in the regular growth conditions according to the description in method. After 24 h (hrs), 48 h and 72 h, crystal violet staining was used to check the proliferation in all groups. For HCC SMMC7721 cell-line, the observation on 24 h application of the Col exhibited proliferation suppression. The differences at 20 μm and 30 μm of the Col concentration showed significantly (Fig. 1A left and B left, both $p < 0.05$). The differences at 40 μm and 50 μm of the Col concentration showed very significant differences as suppression on proliferation (Fig. 1A left and B left, both $p < 0.01$). While the 48 h application of the Col on the cells, this suppression on proliferation was significant at 20 μm of the Col (Fig. 1A left and B left, both $p < 0.05$), and the differences at 30 μm, 40 μm and 50 μm of the Col were very significant (Fig. 1A left and B left, both $p < 0.01$). When the 72 h application on the cells, except the 10 μm of the Col concentration, the other four concentration provided the highest suppression (Fig. 1A left and B left, all $p < 0.01$). It is clear that the 10 μm of the Col concentration applied in medium does not affect the growth of the HCC SMMC7721 (Fig. 1A left and B left, all $p > 0.05$). At other four concentrations from 20 μm, 30 μm, 40 μm to 50 μm, the applied col. dramatically suppressed the proliferation of the HCC SMMC7721.

For HCC HepG2 cell-line, the 24 h application of the Col exhibited suppression on proliferation as well, compared to their control similar to its effect on SMMC7721 cells. The differences at 40 μm of the Col concentration showed significant initially (Fig. 1A middle and B meddle, $p < 0.05$). The differences at 50 μm of the Col concentration showed very significant different suppression on proliferation (Fig. 1A middle and B middle, $p < 0.01$). While the 48 h application on the cells, this suppression on proliferation was significant at 30 μm of the Col (Fig. 1A middle and B middle, $p < 0.05$), and the differences at 40 μm and 50 μm of the Col were very significant (Fig. 1A middle and B middle, both $p < 0.01$). When the 72 h application on the cells, except the 10 μm and 20 μm of the Col concentration, the other three concentration provided the highest suppression (Fig. 1A left and B left, all $p < 0.01$). At other three concentrations from 30 μm, 40 μm to 50 μm, the applied col. dramatically suppressed the proliferation of the HCC HepG2, and the suppression effect on the HepG2 cells is greater than that of the SMMC7721 cell.

The suppression effect on for HCC Hep3B cell-line is similar to that for HepG2 cell-line. For HCC Hep3B cell-line, the 24 h application of the Col presented suppression on proliferation as well compared to their control similar to its effect on HepG2 cells. The differences at 30 μm of the Col concentration showed significant suppression (Fig. 1A right and B right, $p < 0.05$). The differences at 40 μm and 50 μm of the Col concentration presented very significant suppression on proliferation (Fig. 1A right and B right, both $p < 0.01$). While the 48 h application on the cells, this suppression on proliferation was significant at 30 μm of the Col (Fig. 1A right and B right, $p < 0.05$), and the differences at 40 μm and 50 μm of the Col were very significant (Fig. 1A right and B right, both $p < 0.01$). When application hours reached at 72 h, the suppression of Col at the 30 μm, 40 μm and 50 μm of the concentrations all reach at highest level (Fig. 1A right and B right, all $p < 0.01$). It is clear that the 10 μm and 20 μm of the Col concentration applied in medium does not affect the growth of the HCC Hep3B. Just like the HCC HepG2, at other three concentrations from 30 μm, 40 μm to 50 μm, the applied col. dramatically suppressed the proliferation of the HCC Hep3B, and the suppression effect on the Hep3B cells are greater than that of the SMMC7721 cell and equal to the effect of the HepG2.

From our data presented, our study firmly approved that, at least in HCC SMMC7721, HepG2 and Hep3B cell-line cultures, the columbamine clearly inhibited the cell proliferation with its solid effect on HCC cell proliferation within *in vitro* culture system.

3.2. Columbamine stroked the growth of HCC cells and applied suppression on tumorigenesis in animal

In order to confirm the suppression effect on cell proliferation and *in-vivo* inhibition on tumor growth, we applied *in vitro* HCC SMMC7721 colony-growth test, and animal tumorigenesis with three different concentrations at Col low-dosage of 30 μm, at medium-dosage of 40 μm, and at high-dosage of 50 μm.

HCC SMMC7721 cells were grown in the routine condition and treated with columbamine at the low-dosage, the medium-dosage and the high-dosage for continuous maintenance till colonies formed. This striking suppression on the SMMC7721 cell growth is not only performed according to the colony-number decrease (Fig. 1C), but also are representative with PCNA molecular marker (Fig. 1D). The 30 μm of the Col treatment showed no significant difference ($p > 0.05$), but the 40 μm of the Col treatment performed very significant suppression ($p < 0.01$), and the 50 μm of the Col carried out dramatic significance ($p < 0.001$) when normalized to the bland control. Compared to non-treatment and DMSO-treatment, the columbamine suppression on the HCC SMMC7721 is perceptibly dosage-dependent.

In the *in vitro* cellular level, columbamine suppresses the growth or proliferation of HCC within culture system as exhibited above. In order to fulfill its possible clinic provisional, we inspected the drug within *in vivo* tumorigenesis in animal model. As similar to the colony growth experiment, Col treatments with low-dosage of 5 mg/kg, medium-dosage of 10 mg/kg and high-dosage of 20 mg/kg were utilized in the mice with the direct-feeding procedure described in Material and methods. These three-dosage groups along with non-treatment control groups were inspected in the period of 21 days for the *in vivo* animal experiments (Fig. 1E).

As usual in non-treatment control groups, seeded HCC SMMC7721 tumor-cells grew and were able to be observed at 7th day after seeding, and then experienced six-day stable phase of the preliminary growth period. Sequentially, the tumor growth speeded up rapidly up to about 1 cm^3 in size at the end of 21 days. When the low-dosage treated with

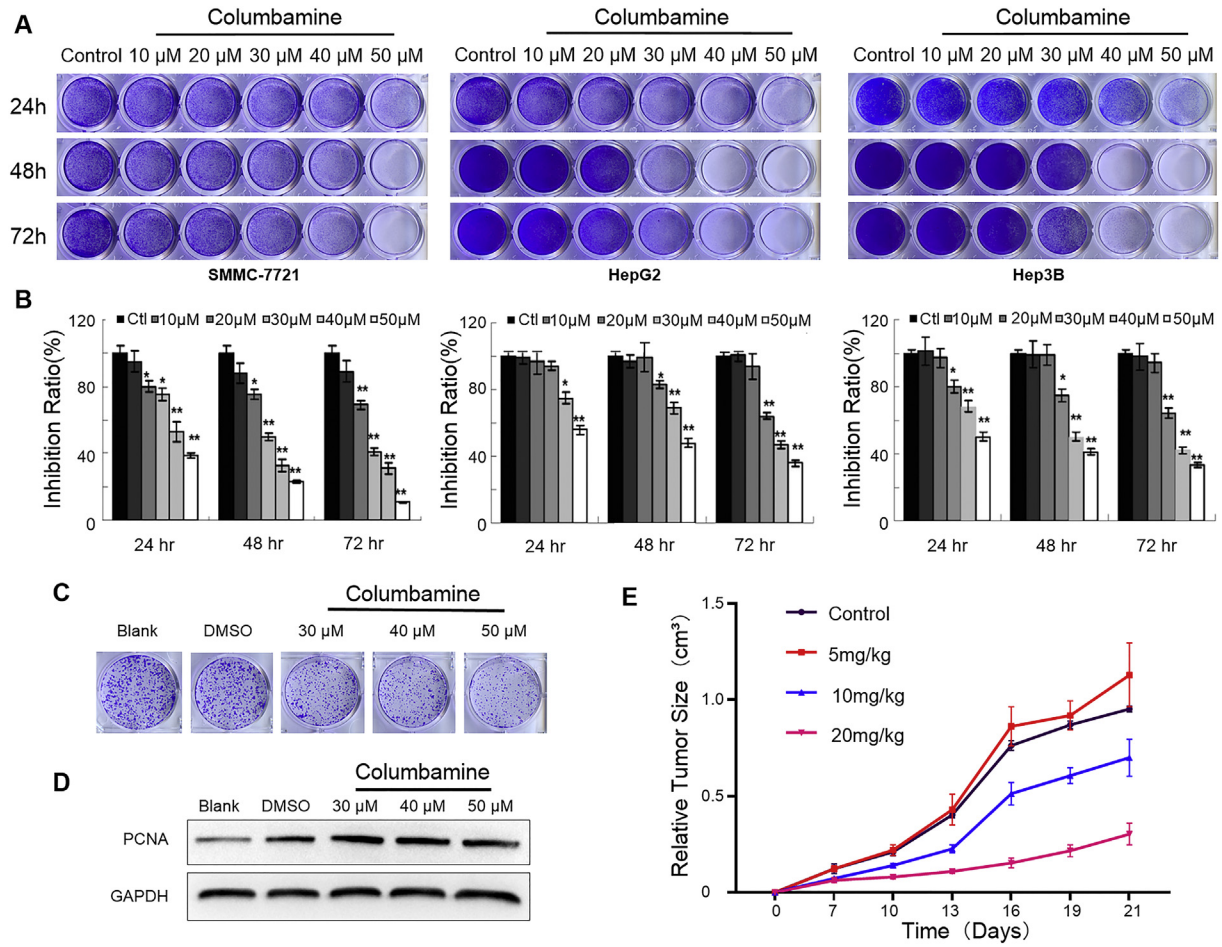

Fig. 1. The inhibition effects of Columbamine on proliferation of HCC cells including SMMC7721, HepG2 and Hep3B. Panel A shows the crystal violet staining of HCC cell lines (SMMC7721, HepG2 and Hep3B) after cultured in the concentration of 10 μM, 20 μM, 30 μM, 40 μM and 50 μM for 24 h, 48 h and 72 h. Panel B show the relative growth rate of each well in panel A. Panel C shows the growth of colony formation assay of SMMC7721 cells with DMSO, 30 μM, 40 μM and 50 μM Col. Panel D displays the PCNA expression of the colonies in panel C by Western blot. The blotted PCNA protein was normalized to GAPDH. Panel E present the relative tumor growth curve of *Nude Mouse* ($n \geq 12$ for each groups including 5 mg/kg, 10 mg/kg, 20 mg/kg and 0 mg/kg control groups) injected with SMMC7721 cells in subcutaneous tissues. Different Col dosages (5 μM, 10 μM and 20 mg/kg) were applied in these *Nude Mouse*. $^{**}p < 0.01$; $^{*}p < 0.05$. (For interpretation of the references to colour in this figure legend, the reader is referred to the web version of this article.)

the animals, there was no significant effect on the tumor growth. However, when the medium-dosage Col was applied on the tumorigenic mice, the tumor growth was dramatically limited. The stable phase of the preliminary growth period lasted to 13 days and then the tumor came to the fast growth phase. At the end of 21 days, the tumor size reached at 75% of the non-treated tumor size. In the high-dosage group, the suppression strongly limited the tumor growth by eliminating the fast growth phase. The growth maintained in the stable phase of the preliminary growth period in the entire inspection period, and the end-up size of the tumor only reached at 25% of the non-treated tumor at the 21 days (Fig. 1E). The medium- and high-dosage compared to low-dosage Col can be dramatically effective on the tumor growth over the non-treatment in the preliminary growth phase and the rapid growth phases.

Therefore, according to our experiments above, columbamine can effectively suppress the proliferation of HCC SMMC7721 and firmly inhibit the tumor-growth. The suppression function of columbamine is dosage-dependent on the *in vitro* cell culture system and *in-vivo* animal model, which provides strong potential for clinic application.

3.3. Columbamine inhibits the migration and invasion on HCC cells with dosage-dependency

Migration and invasion are major two physiognomies which characterize tumor cells as carcinoma in cellular physiological behaviors. To identify cellular mechanism of columbamine suppression on HCC, we further investigated alternation of the cell behaviors with inspection on wound healing, migration and invasion procedures when the Col treatments were applied on SMMC7721 and HepG2.

The wounds were generated in both cultured HCC SMMC7721 and HepG2 *in vitro* with low concentration of (10 μm), medium concentration (20 μm) and high concentration (30 μm) of columbamine plus the control group without Col treatment as the healing process would last. After 24-hour culture, compared to the non-treatment group, all three dosage for SMMC7721 exhibited significant delay on their healing processes. For the wound healings among the groups of the low concentration, the medium concentration and the high concentration, the wound-gap width in the high concentration group was recovered at the slowest speed and left the width as the widest compared to other Col groups. The wound-gap width in the low concentration group was filled with the cells at fast speed, and the width left open with the similar area to the non-treatment control (Fig. 2A).

Process of the wound healing in cultured HCC HepG2 appeared the similar effect on the wound-gap. The HepG2 cells in the high Col concentration filled the width of wound-gap at the slowest speed with existence of a few cells in the gap and left more space unoccupied. The cells in the low Col concentration filled the width of wound-gap at the fast speed with more cells appearance in the gap (Fig. 2B). It is

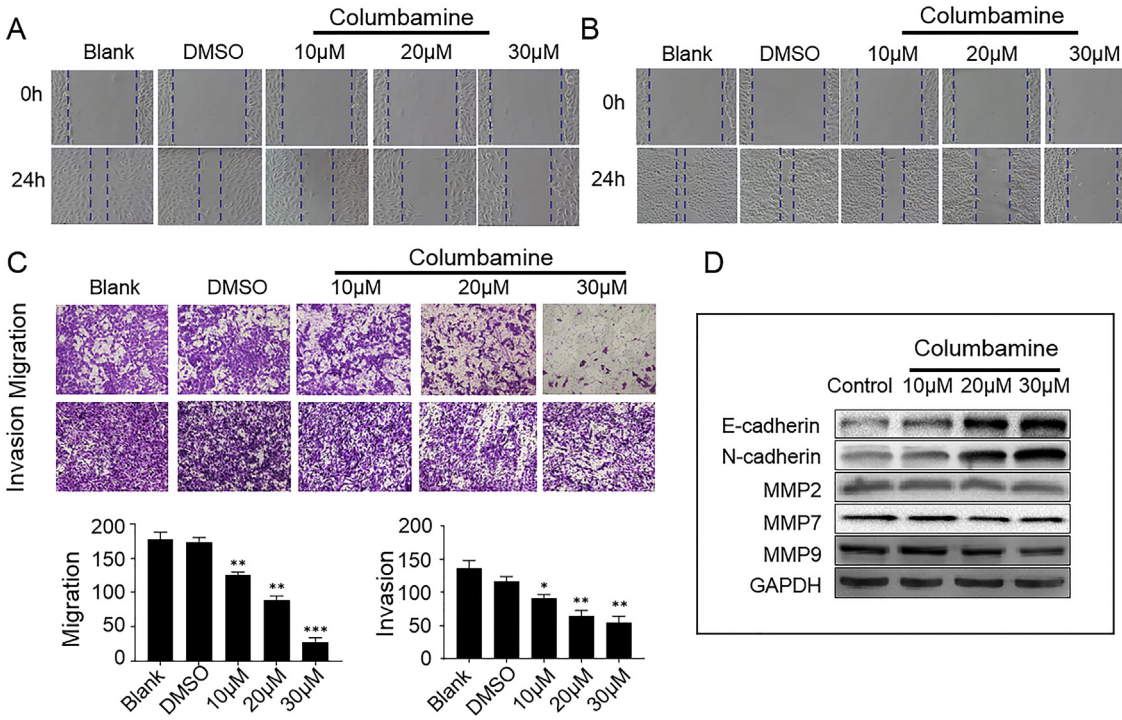

Fig. 2. The inhibition effects of Columbamine on migration and invasion of HCC cells. Panel A and B display the migration of SMMC7721 and HepG2 cells with 10 μM, 20 μM and 30 μM Col at 0 h and 24 h after wound healing. The green lines show the gap distance of cell wound. Panel C shows the inhibition effect Col (10 μM, 20 μM and 30 μM) on migration and invasion of SMMC7721 cells through Transwell experiments (with and without ECM). Panel D shows the proteins expression of migration and invasion related E-Cadherin, N-Cadherin, MMP2, MMP7 and MMP9 in SMMC7721 cells after growing in 30 μM, 40 μM and 50 μM Col for 36 h. All blotted proteins were normalized to GAPDH. (For interpretation of the references to colour in this figure legend, the reader is referred to the web version of this article.)

acceptable that the width indicating between two green lines is the credible meaning of the cell migrating towards the wound-gap from the full cell-confluence area beyond two lines. Based on these experiments, it is confident to conclude that the Col suppression on the HCC controlled their cellular behavior on the inhibiting migration.

Normally, alternation on invasion of the carcinoma cells is accompanied by migration with tumor development in both *in vitro* and *in vivo* systems. Indeed, in our experiments with HCC SMMC7721 *via* transwell, the following phenomenon was observed as well. In the high Col concentration group, less SMMC7721 cells invaded through transwell-membrane. Appositively, in the low Col concentration group, more SMMC7721 cells run through the membrane, and the cells in the medium concentration group were documented in the between (Fig. 2C). According to our experiments, it is conspicuous that Col inhibition on the migration and invasion of HCC SMMC7721 and HepG2 cells are dosage-dependent *in vitro*.

It is normally considered that any alternation of cellular behaviors would involve in molecular alternation in cells mainly concerning related proteins. Therefore, we further employed antibodies of invasion markers including E-cadherin, N-Cadherin, MMP2, MMP7 and MMP9. Our results demonstrated that, with the suppression of columbamine on HCC cells and SMMC7721 generated tumors in animal model, the inhibition effect is accompanied with significant alternations of cell-membrane integrated proteins *i.e.* the up-regulation of E-cadherin and down-regulation of N-cadherin. The extracellular matrix proteins are also examined with the results of the down-regulation of MMP2 and MMP7 accompanying with the no significant change at expression level of MMP9 (Fig. 2 D). All above results in Western blotting analysis were normalized to GAPDH.

3.4. Columbamine induces apoptosis in cultured HCC cells in vitro

In order to explore the fate of HCC cells after the columbamine suppression, we inspected suppressed cells under the Col treatment. We continuously maintained HCC SMMC7721 in the condition of the treatment at the low concentration of (30 μm), the medium concentration (40 μm) and the high concentration Col (50 μm).

Compared to the non-treatment cells, the SMMC7721 under the high Col concentration exhibited more condensed and fragmented nuclear DNA staining, and the cells under the low Col concentration presented less number of condensed nuclear DNA staining along with the density of the staining under the medium Col concentration (Fig. 3A). The cell number under at 30 μm, 40 μm and 50 μm of Col concentration exhibited dramatic increasing with increase of the Annexin positive cells from 6.87% at the low-dosage, *via* 11.3% at the medium-dosage, and up to 18% at the high-dosage (Fig. 1C, all $p < 0.01$) in comparison to 4.34% in the control (Fig. 3B). In order to identify if these condensed nuclear DNA are under apoptosis, we examined a series of the marker proteins of apoptosis on these Col treated HCC SMMC7721 including Caspase3/Cleaved caspase3, PAPR/Cleaved PAPR, BCL2 and BAD normalized to GAPDH with Western Blotting analysis.

As two pared of the apoptotic marker proteins, the cleaved caspase3 and the cleaved PAPR perform representative of apoptotic cells. With the increase of columbamine from the low Col concentration *via* the medium Col concentration to the high Col concentration, the expression of the cleaved caspase3 and the cleaved PAPR dramatically increased in comparison to the non-detectable protein level in the non-Col treatment control cells, along with the stable expression of their original Caspase3 and PAPR proteins in the four groups. Meanwhile, the Col treatments at the low, medium and high concentrations also led to the down-expression of BCL2 and synchronic up-expression of BAD (Fig. 3 C).

According to the staining on the condensed nuclear DNA after the Col treatment combined with the results representative alternation of apoptotic marker Caspase3/Cleaved caspase3, PAPR/Cleaved PAPR, BCL2 and BAD, we would like to claim that columbamine induces

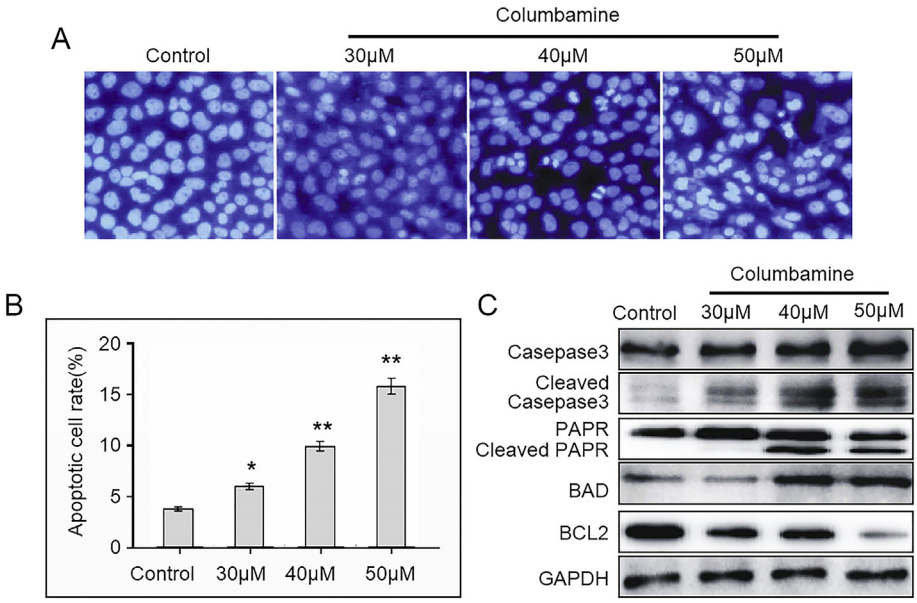

Fig. 3. Programmed apoptosis of HCC cells induced by Columbamine. Panel A and B present the Hoechst 33258 staining and Annexin V/PI staining applied on SMMC7721 cells after treatment with 30 μM, 40 μM and 50 μM Col for 24 h, respectively. The phenomenon of nucleus pyknosis and karyorrhexis are displayed in panel A and the percent of Annexin positive cells are shown in panel B. Panel C shows the expression of apoptosis related proteins including Caspase3, Cleaved caspase3, PAPR, Cleaved PAPR, BCL2 and BAD in SMMC7721 cells after growing in 30 μM, 40 μM and 50 μM Col for 36 h. All blotted proteins were normalized to GAPDH. $^{**}p < 0.01$; $^{*}p < 0.05$.

apoptosis in cultured HCC SMMC7721 cells *in vitro* resulting suppression on tumor growth.

3.5. Columbamine promoted suppression is associated with PI3K/AKT, p38 and ERK1/2 signaling in HCC cells

For comprehensive understanding of molecular mechanism on columbamine promoted suppression for the tumorigenesis, we scrutinized potential pathways on hepatocellular carcinoma. Bufalin, as a Chinese traditional medicine, is a cardiotonic steroid extracted from the Chinese toad venom [27] and its pharmacology function is currently studied. The recent data reported that bufalin can suppress the growth of hepatocellular carcinoma. By conquering invasion and metastasis of the HCC cells, the bufalin suppression on liver and lung cancers targeted on HIF-1α *via* the PI3K/AKT/mTOR pathway [28–30], one of the major calcium signaling related pathways [14]. Therefore, we inspected the columbamine promoted suppression on HCC in nude mice and then tested the relevant pathways subsequently.

Focusing on calcium related pathways, we applied Western Blotting analysis plus quantitative statics to inspect the components of PI3K/AKT, p38 and ERK1/2 signaling pathways to discover the molecular pathways regarding to columbamine promoted suppression on the HCC cells and SMMC7721 originated tumor in nude mice. The antibodies recognizing the following proteins were included as AKT along with its phosphorylated configuration p-AKT (Ser473) and p-AKT (Thr308) controlled by PTEN, p38 and ERK1/2 along with their phosphorylated configuration p-p38 and p-ERK1/2. All blotted proteins were normalized to GAPDH.

Three groups were set as the Col treatment condition at the low concentration of (30 μm), the medium concentration (40 μm) and the high concentration (50 μm) in the cultured HCC SMMC7721. It is not surprised that the expression of PTEN was retrieved in the dosage-dependent manner after the Col applied in the medium because of the columbamine suppression function on the HCC cells and the cell originated tumor in nude mice. Along with non-changing pattern of AKT expression under the low-, medium- and high-concentration, both expressions of phosphorylated AKTs, p-AKT(Ser473) and p-AKT(Thr308), decreased significantly (Fig. 4A and C). Our data would like to conclude that the Col suppression on HCC is associated with PI3K/AKT pathway accompanying with PTEN rebooting.

Under the treatment condition of the low-, medium- and high-concentration of columbamine, both ERK1/2 and p38 exhibited no significant on their expression. However, we unexpectedly found that the expressions of their phosphorylated configuration p-ERK1/2 were significant declined, and p-p38 was dramatically decreased individually (Fig. 4B and D). This data could be pointed that the Col suppression on HCC is concomitant to MAPK pathway association PTEN to reboot after the Col treatments. Evidently, these PI3K/AKT and MAPK pathways outline the molecular mechanism of the columbamine promoted suppression on HCC cells and liver tumors in animal model.

4. Discussion

Using *in vitro* culture system, our data approved that columbamine suppressed the proliferation of hepatocellular carcinoma cells including HCC SMMC7721, HepG2 and Hep3B, and decreases the growth of HCC SMMC7721 induced tumor *in vivo* by subcutaneous injection in nude mice. The columbamine suppression affects the HCC cells *via* deducing the movement of their migration and invasion indicated with the up-expression of E-cadherin and the down-expression of MMP2, and MMP9. Meanwhile, the suppressed cells fate through apoptotic process in cellular level indicated with the up-expression of the cleaved Caspase3, cleaved PAPR and BAD, and the down-expression of BCL2 protein. Furthermore, we demonstrated that the columbamine suppression on HCC growth is associated with PI3K/AKT and MAPK pathways. This molecular mechanism unveiled by our results is confident since these pathways are associated with normal proliferation and tumorigenesis approved by many studies [14,16,31–33]. As an intracellular calcium chelator BAPTA-AM plays inhibition on p38 MAPK and Akt pathways, it is possible that our result could lead current research to cellular calcium signaling system [34].

We would like to consider that our result is comprehensive for understanding hepatocellular carcinoma as that the columbamine promoted suppression is mainly based on three HCC cell lines, HCC SMMC7721 [35,36], HepG2 and Hep3B [37–40], which all are the most representative cell lines for HCC currently. HCC SMMC7721 possess capability in the processes of hepatocarcinoma genesis, growth and metastasis with its six clusters of novel protein profile including mitofilin, ERp29, UC-cytochrome C reductase core protein I, peroxisomal CoA hydratase, p-4 and p-3-o CoA transferase 1 precursor, which normally employed to investigate HCC proliferation and invasion in recent study [35,36]. HCC HepG2 and Hep3B cell lines are commonly used to inspect hepatocellular carcinoma which most likely originated from Hepatitis virus pathogenesis [37–40]. Therefore, our results should

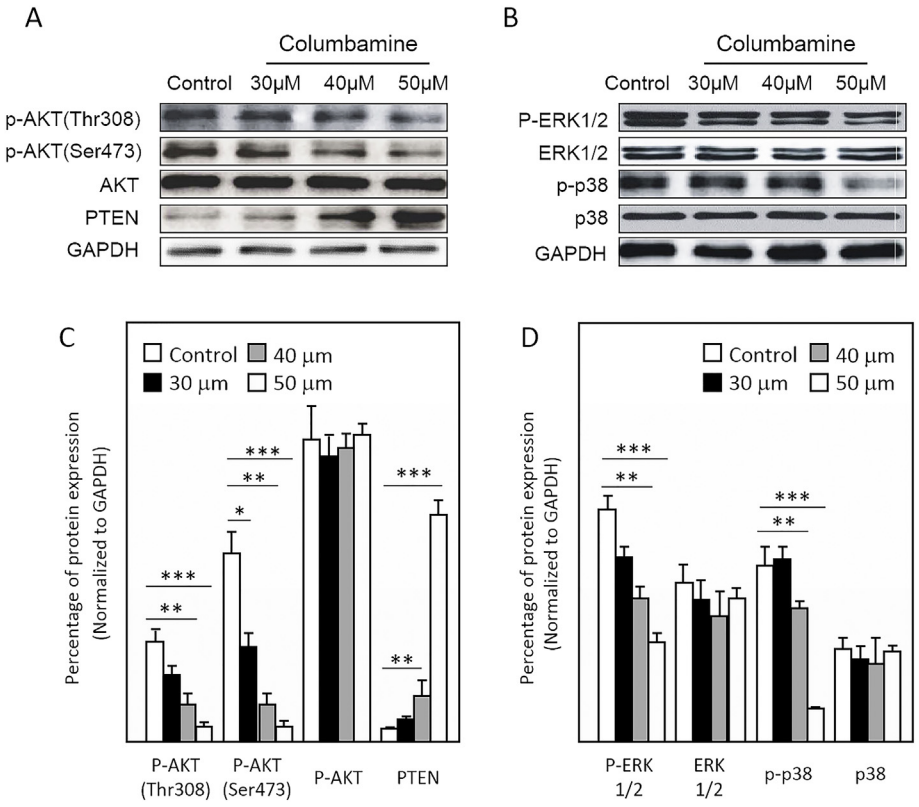

Fig. 4. The Columbamine suppression on HCC cells is associated with PI3K/AKT and MAPKs signal pathways. Panel A shows the expression of AKT, p-AKT(Ser473), p-AKT(Thr308) and PTEN proteins of PI3K/AKT pathway in SMMC7721 cells after cultured in 30 μM, 40 μM and 50 μM Col for 36 h. Panel B presents the expression of p38, ERK1/2, p-p38 and p-ERK1/2 proteins of MAPKs pathway. Panels C and D are corresponding to Panels A and B individually. All blotted proteins were normalized to GAPDH expression. ***$p < 0.001$; **$p < 0.01$; *$p < 0.05$.

cover the most categories of hepatocarcinoma genesis.

According to our results, SMMC7721 cells exhibited much dramatic difference between migration and invasion with Col treatment at the concentration of 10 μm, 20 μm and 30 μm (Fig. 2C). The data suggested that the columbamine suppression on tumor growth affected on cell migration first, and then weaken the invasion of the SMMC7721 cells. From our key data show in Fig. 1, we decided not to use full-spectrum concentrations because at the 50 μm as the highest concentration, we could not obtain enough cells for further analysis. According to our experiments, only less cells could be observed at this end-stage in Fig. 2C. As we discovered in Fig. 4 A, the increasing expression of PTEN as the well-recognized tumor suppressing protein, confirmed that the columbamine suppression could play the role through PTEN pathway.

Our data showed that Columbamine suppression slowed-down the migration, invasion, and led to program cell death as we presented above. It is rational that the suppression first change p38 MAPK and Akt pathways led to irregular calcium signaling. The involvement of the irregular calcium affected on cell behaviors by limiting its migration and invasion capability. Eventually, the cell decided their fate to programmed death *i.e.* apoptosis. For further study for Columbamine suppression on HCC growth, we would like to perform on two major issues. One issue aims inspecting the suppression effect within *in vivo* HCC experiments, and other issue will be focusing on procedure of columbamine delivery efficiency in HCC animal model.

Traditional medicine has been played marvelous role on strengthening human health against life-threatening diseases. For insistence, artemisinin, originally extracted from the herb plant *Artemisia annua*, and derivatives dihydroartemisinin, artesunate and artemether are commonly used in the clinic treatments for anti-malarial for years [41–43]. Millions of lives have been saved since its application worldwide. The discovery on the application of these medicines has been encouraging many researches working on traditional medicine against cancers and other overwhelming diseases. Functional investigation on columbamine could be one of the best subjects that the most attention should be settled on. According to the data presented in here, dramatic HCC suppression on both cell-growth limitation from *in vitro* cell-culture against proliferation, migration and invasion, and tumor-growth inhibition from the data obtained from animal tumor model originated from HCC cell line, we claim that the columbamine promoted inhibition on HCC worth concentrated works posterior to its application on clinic trial.

Abbreviations

Col	Columbamine
HCC	Hepatocellular carcinoma
AFP	alpha-fetoprotein
HDF	human dermal fibroblasts
CaSR	calcium-sensing receptor
IP3R	inositol 1,4,5-trisphosphate receptor
PBS	phosphate buffered saline
PI	propidium iodide
PFA	paraformaldehyde
PVDF	polyvinylidene difluoride
FBS	fetal bovine serum
EMC	ectracellular matrix protein
FITC	Fluorescein isothiocyanate
BAPTA-AM	(1,2-bis(o-amino phenoxy)ethane-N,N,N′,N′-tetraacetic acid)

Competing interests

The authors declare that they have no competing interests.

Authors' contributions

SL conceived of the study. ZL, SL, LZ, ZY, XC, ZC, HY, CZ, CZ and WL developed protocols, collected and analyzed all data. WL, ZL, SL, LZ and CZ prepared the manuscript, and all authors edited the manuscript. All authors read and approved the final manuscript.

Availability of data and materials

Not applicable.

Consent for publication

Not applicable.

Ethics approval and consent to participate

All applicable international, national, and/or institutional guidelines for the care and use of animals were followed.

Acknowledgements

This work was supported by the internal support for distinguished professor of the university (#MCR2017030983), and the China Ministry of Education (#GK20160100) to SL, Outstanding Student Award on post-graduation study to ZL (#X2017YS002) and PG (#X2017YS043).

References

[1] A. Forner, J.M. Llovet, J. Bruix, Hepatocellular carcinoma, Lancet (London, England) 379 (2012) 1245–1255, https://doi.org/10.1016/s0140-6736(11)61347-0.
[2] M.C. Wallace, D. Preen, G.P. Jeffrey, et al., The evolving epidemiology of hepatocellular carcinoma: a global perspective, Expert Rev. Gastroenterol. Hepatol. 9 (2015) 765–779, https://doi.org/10.1586/17474124.2015.1028363.
[3] I. Saeki, T. Yamasaki, M. Maeda, et al., Treatment strategies for advanced hepatocellular carcinoma: Sorafenib vs hepatic arterial infusion chemotherapy, World J. Hepatol. 10 (2018) 571–584, https://doi.org/10.4254/wjh.v10.i9.571.
[4] J.K. Heimbach, L.M. Kulik, R.S. Finn, et al., AASLD guidelines for the treatment of hepatocellular carcinoma, Hepatology 67 (2018) 358–380, https://doi.org/10.1002/hep.29086.
[5] F. Pinero, J. Poniachik, E. Ridruejo, et al., Hepatocellular carcinoma in Latin America: diagnosis and treatment challenges, World J. Gastroenterol. 24 (2018) 4224–4229, https://doi.org/10.3748/wjg.v24.i37.4224.
[6] A. Colli, M. Fraquelli, G. Casazza, et al., Accuracy of ultrasonography, spiral CT, magnetic resonance, and alpha-fetoprotein in diagnosing hepatocellular carcinoma: a systematic review, Am. J. Gastroenterol. 101 (2006) 513–523, https://doi.org/10.1111/j.1572-0241.2006.00467.x.
[7] K.W. Ma, T.T. Cheung, Surgical resection of localized hepatocellular carcinoma: patient selection and special consideration, J. Hepatocell. Carcinoma. 4 (2017) 1–9, https://doi.org/10.2147/JHC.S96085.
[8] S.F. Ang, E.S. Ng, H. Li, et al., The Singapore Liver Cancer Recurrence (SLICER) score for relapse prediction in patients with surgically resected hepatocellular carcinoma, PLoS One 10 (2015) e0118658, , https://doi.org/10.1371/journal.pone.0118658.
[9] M. Bao, Z. Cao, D. Yu, et al., Columbamine suppresses the proliferation and neovascularization of metastatic osteosarcoma U2OS cells with low cytotoxicity, Toxicol. Lett. 215 (2012) 174–180, https://doi.org/10.1016/j.toxlet.2012.10.015.
[10] R.K. Santhanam, S. Ahmad, F. Abas, et al., Bioactive constituents of zanthoxylum rhetsa bark and its cytotoxic potential against B16-F10 melanoma cancer and normal human dermal fibroblast (HDF) cell lines, Molecules 21 (2016), https://doi.org/10.3390/molecules21060652.
[11] L.L. Zhang, L.N. Ma, D. Yan, et al., Dynamic monitoring of the cytotoxic effects of protoberberine alkaloids from Rhizoma Coptidis on HepG2 cells using the xCELLigence system, Chin. J. Nat. Med. 12 (2014) 428–435, https://doi.org/10.3724/Sp.J.1009.2014.00428.
[12] Y. Zhou, S.J. Cao, Y. Wang, et al., Berberine metabolites could induce low density lipoprotein receptor up-regulation to exert lipid-lowering effects in human hepatoma cells, Fitoterapia 92 (2014) 230–237, https://doi.org/10.1016/j.fitote.2013.11.010.
[13] X.H. Xu, S.P. Balk, W.B. Isaacs, et al., Calcium signaling: an underlying link between cardiac disease and carcinogenesis, Cell Biosci. 8 (2018), https://doi.org/10.1186/s13578-018-0236-0 ARTN 39.
[14] M. Xu, A. Seas, M. Kiyani, et al., A temporal examination of calcium signaling in cancer- from tumorigenesis, to immune evasion, and metastasis, Cell Biosci. 8 (2018) 25, https://doi.org/10.1186/s13578-018-0223-5.
[15] J. Humeau, J.M. Bravo-San Pedro, I. Vitale, et al., Calcium signaling and cell cycle: progression or death, Cell Calcium 70 (2018) 3–15, https://doi.org/10.1016/j.ceca.2017.07.006.
[16] L.Y. Wang, M.M. Xu, Z.G. Li, et al., Calcium and CaSR/IP3R in prostate cancer development, Cell Biosci. 8 (2018), https://doi.org/10.1186/s13578-018-0217-3 ARTN 16.
[17] A. Bononi, C. Giorgi, S. Patergnani, et al., BAP1 regulates IP3R3-mediated ca(2+) flux to mitochondria suppressing cell transformation, Nature 546 (2017) 549–553, https://doi.org/10.1038/nature22798.
[18] S. Kuchay, C. Giorgi, D. Simoneschi, et al., PTEN counteracts FBXL2 to promote IP3R3- and ca(2+)-mediated apoptosis limiting tumour growth, Nature 546 (2017) 554–558, https://doi.org/10.1038/nature22965.
[19] L. Guo, L. Wang, R. Yang, et al., Optimizing conditions for calcium phosphate mediated transient transfection, Saudi J. Biol. Sci. 24 (2017) 622–629, https://doi.org/10.1016/j.sjbs.2017.01.034.
[20] B. Tang, B. Lei, G. Qi, et al., MicroRNA-155-3p promotes hepatocellular carcinoma formation by suppressing FBXW7 expression, J. Exp. Clin. Cancer Res. 35 (2016) 93, https://doi.org/10.1186/s13046-016-0371-6.
[21] X. Zhou, M. Xu, L. Wang, et al., Liver-specific NG37 overexpression leads to diet-dependent fatty liver disease accompanied by cardiac dysfunction, Genes Nutr. 11 (2016) 14, https://doi.org/10.1186/s12263-016-0529-z.
[22] X. Xu, M.B. Bhat, M. Nishi, et al., Molecular cloning of cDNA encoding a drosophila ryanodine receptor and functional studies of the carboxyl-terminal calcium release channel, Biophys. J. 78 (2000) 1270–1281, https://doi.org/10.1016/S0006-3495(00)76683-5.
[23] J. Espada, M. Matabuena, N. Salazar, et al., Cryptomphalus aspersa mollusc eggs extract promotes migration and prevents cutaneous ageing in keratinocytes and dermal fibroblasts in vitro, Int. J. Cosmet. Sci. 37 (2015) 41–55, https://doi.org/10.1111/ics.12167.
[24] M.C. Cruz, F. Sanz-Rodriguez, A. Zamarron, et al., A secretion of the mollusc *Cryptomphalus aspersa* promotes proliferation, migration and survival of keratinocytes and dermal fibroblasts in vitro, Int. J. Cosmet. Sci. 34 (2012) 183–189, https://doi.org/10.1111/j.1468-2494.2011.00699.x.
[25] Y. Hu, Q. Yu, Y. Zhong, et al., Silencing ELMO3 inhibits the growth, invasion, and metastasis of gastric cancer, Biomed. Res. Int. 2018 (2018) 3764032, https://doi.org/10.1155/2018/3764032.
[26] X. Wang, F.H. Pang, L. Huang, et al., Synthesis and biological evaluation of novel dehydroabietic acid-oxazolidinone hybrids for antitumor properties, Int. J. Mol. Sci. 19 (2018), https://doi.org/10.3390/ijms19103116.
[27] M. Okada, T. Suga, Pharmacology of the principles isolated from Senso (Ch'an Su) the dried venom of the Chinese toad (IV), Asian Med. J. 3 (1960) 155–160.
[28] H. Wang, C. Zhang, L. Xu, et al., Bufalin suppresses hepatocellular carcinoma invasion and metastasis by targeting HIF-1alpha via the PI3K/AKT/mTOR pathway, Oncotarget 7 (2016) 20193–20208, https://doi.org/10.18632/oncotarget.7935.
[29] Z.J. Zhang, Y.K. Yang, W.Z. Wu, Bufalin attenuates the stage and metastatic potential of hepatocellular carcinoma in nude mice, J. Transl. Med. 12 (2014), https://doi.org/10.1186/1479-5876-12-57 Artn 57.
[30] S.H. Wu, T.Y. Wu, Y.T. Hsiao, et al., Bufalin induces cell death in human lung cancer cells through disruption of DNA damage response pathways, Am. J. Chin. Med. 42 (2014) 729–742, https://doi.org/10.1142/S0192415x14500475.
[31] W. Dai, Y. Bai, L. Hebda, et al., Calcium deficiency-induced and TRP channel-regulated IGF1R-PI3K-Akt signaling regulates abnormal epithelial cell proliferation, Cell Death Differ. 21 (2014) 568–581, https://doi.org/10.1038/cdd.2013.177.
[32] D. Horn, J. Hess, K. Freier, et al., Targeting EGFR-PI3K-AKT-mTOR signaling enhances radiosensitivity in head and neck squamous cell carcinoma, Expert Opin. Ther. Targets 19 (2015) 795–805, https://doi.org/10.1517/14728222.2015.1012157.
[33] J. Polivka, F. Janku, Molecular targets for cancer therapy in the PI3K/AKT/mTOR pathway, Pharmacol. Ther. 142 (2014) 164–175, https://doi.org/10.1016/j.pharmthera.2013.12.004.
[34] S. Zhou, X. Yuan, Q. Liu, et al., BAPTA-AM, an intracellular calcium chelator, inhibits RANKL-induced bone marrow macrophages differentiation through MEK/ERK, p38 MAPK and Akt, but not JNK pathways, Cytokine 52 (2010) 210–214, https://doi.org/10.1016/j.cyto.2010.07.003.
[35] Y. Feng, Z.M. Tian, M.X. Wan, et al., Protein profile of human hepatocarcinoma cell line SMMC-7721: identification and functional analysis, World J. Gastroenterol. 13 (2007) 2608–2614, https://doi.org/10.3748/wjg.v13.i18.2608.
[36] K. Wang, H.Y. Lim, S. Shi, et al., Genomic landscape of copy number aberrations enables the identification of oncogenic drivers in hepatocellular carcinoma, Hepatology 58 (2013) 706–717, https://doi.org/10.1002/hep.26402.
[37] S.J. Busch, R.L. Barnhart, G.A. Martin, et al., Differential regulation of hepatic triglyceride lipase and 3-hydroxy-3-methylglutaryl-CoA reductase gene expression in a human hepatoma cell line, HepG2, J. Biol. Chem. 265 (1990) 22474–22479.
[38] B.B. Knowles, C.C. Howe, D.P. Aden, Human hepatocellular carcinoma cell lines secrete the major plasma proteins and hepatitis B surface antigen, Science 209 (1980) 497–499.
[39] A.S. Haron, S.S. Syed Alwi, L. Saiful Yazan, et al., Cytotoxic effect of thymoquinone-loaded nanostructured lipid carrier (TQ-NLC) on liver cancer cell integrated with hepatitis B genome, Hep3B, Evid. Based Complement. Alternat. Med. 2018 (2018) 1549805, https://doi.org/10.1155/2018/1549805.
[40] M. Yamaguchi, O. Hankinson, 2,3,7,8Tetrachlorodibenzopdioxin suppresses the growth of human liver cancer HepG2 cells in vitro: involvement of cell signaling factors, Int. J. Oncol. 53 (2018) 1657–1666, https://doi.org/10.3892/ijo.2018.4507.
[41] G. Brown, Artemisinin and a new generation of antimalarial drugs, Educ. Chem. 43 (2006) 97–99.
[42] N.J. White, Assessment of the pharmacodynamic properties of antimalarial drugs in vivo, Antimicrob. Agents Chemother. 41 (1997) 1413–1422.
[43] N.M. Douglas, N.M. Anstey, B.J. Angus, et al., Artemisinin combination therapy for vivax malaria, Lancet Infect. Dis. 10 (2010) 405–416, https://doi.org/10.1016/S1473-3099(10)70079-7.